Triphenylamine-based dyes for dye-sensitized solar cells

ARTICLE *in* DYES AND PIGMENTS · JUNE 2009

Impact Factor: 3.97 · DOI: 10.1016/j.dyepig.2008.10.012

Dyes and Pigments 81 (2009) 224–230

Contents lists available at ScienceDirect

Dyes and Pigments

journal homepage: www.elsevier.com/locate/dyepig

Triphenylamine-based dyes for dye-sensitized solar cells

Fan Zhang [a], Yan-hong Luo [b], Jin-sheng Song [a], Xiao-zhi Guo [b], Wei-li Liu [a], Chun-ping Ma [a], Yong Huang [a], Mao-fa Ge [a], Zhishan Bo [a,*], Qing-Bo Meng [b,**]

[a] Beijing National Laboratory for Molecular Sciences, Institute of Chemistry, Chinese Academy of Sciences, Beijing 100190, China
[b] Beijing National Laboratory for Condensed Matter Physics, Institute of Physics, Chinese Academy of Sciences, P.O. Box 603, Beijing 100190, China

ARTICLE INFO

Article history:
Received 19 July 2008
Received in revised form
16 October 2008
Accepted 20 October 2008
Available online 6 November 2008

Keywords:
Dye-sensitized solar cells
Bis-TPA substituted dyes
Mono-TPA substituted dyes
Donor-acceptor
Higher open-circuit voltage (V_{oc})
Nanocrystallite TiO_2 film

ABSTRACT

Three, novel dyes carrying bis-triphenylamine donor groups were designed and synthesized, and their optical and electrochemical properties were characterized. TiO_2-based dye-sensitized solar cells fabricated with the dyes as photosensitizers displayed higher open-circuit voltage and power conversion efficiency than the corresponding mono-TPA substituted donor-acceptor dyes. The two, hydrophobic bis-triphenylamine donor groups within the dyes effectively inhibited the approach of I_3^- to the surface of nanocrystallite TiO_2 film. The most promising of the novel dyes displayed a power conversion efficiency of 5.06%, short circuit photocurrent density of 10.25 mA cm^{-2}, open circuit photovoltage of 0.678 V and fill factor of 0.73.

1. Introduction

Since Grätzel et al. reported the first efficient dye-sensitized solar cells (DSSCs) in 1991 [1], they have attracted much attention due to their relatively high power conversion efficiency and potentially low cost of production [2–21]. To date, DSSCs with Ru bipyridyl complexes (**N3** and **N719**, their structures are shown in Fig. 1) and the black ruthenium dye as photosensitizers have achieved power conversion efficiencies up to 11.2% and 10.4%, respectively [3,4]. However, the noble metal Ru is a limited resource and is expensive. In order to obtain even cheaper photosensitizer for DSSCs, metal-free organic photosensitizers are strongly desired. Metal-free organic dyes offer superior molar extinction coefficients, low cost, and a diversity of molecular structures. Recently, novel photosensitizers such as coumarin [5], merocyanine [6], cyanine [7], indoline [8], hemicyanine [9], triphenylamine [10–13], dialkylaniline [14], bis(dimethylfluorenyl)aminophenyl [15,16], phenothiazine [17], tetrahydroquinoline [18], and carbazole [19] based dyes have achieved solar-to-electrical power conversion efficiencies up to 5–9%. The main reason for the low conversion efficiency of DSSCs is the low open-circuit voltage (V_{oc}) [20], which is far below the theoretical maximum [21]. Compared with Ru polypyridyl complexes, the V_{oc} of organic dyes for DSSCs is much lower under the same testing condition [10,11]. Charge recombination at the nanocrystallite/dye/redox electrolyte interface restricts the open-circuit voltage [22,23]. For a higher photovoltage and a higher conversion efficiency, the charge recombination process at the interface should be retarded [20,22–24]. The recombination of the injected conduction-band electrons with the oxidized dye molecules and the redox species in the electrolyte are two possible recombination pathways. It has been confirmed that the charge recombination process can be retarded by a larger physical separation of the dye cation state from the surface of nanocrystallite film [25,26].

An efficient dye is usually designed to be of donor-conjugated bridge-acceptor structure called donor–acceptor architecture. Most dye molecules have only one donor group [5,15–18], few have two electron-donating groups [12,13]. In this paper, we have designed and synthesized a novel class of dyes carrying two donor groups, and structures of the novel dyes that possess a donor–acceptor unit with a supplementary non-conjugating donor group dyes are shown in Fig. 1. The novel dyes were fully characterized and applied to the fabrication of DSSCs. The novel dyes have higher open-circuit voltage and power conversion efficiency than the corresponding simple donor–acceptor dyes. The highest power conversion efficiency of DSSC with **2b** is up to 5.06%.

* Corresponding author. Tel./fax: +86 10 8261 8587.
** Corresponding author. Tel./fax: +86 10 8264 9005.
E-mail addresses: zsbo@iccas.ac.cn (Z. Bo), qbmeng@aphy.iphy.ac.cn (Q.-B. Meng).

0143-7208/$ – see front matter © 2008 Elsevier Ltd. All rights reserved.
doi:10.1016/j.dyepig.2008.10.012

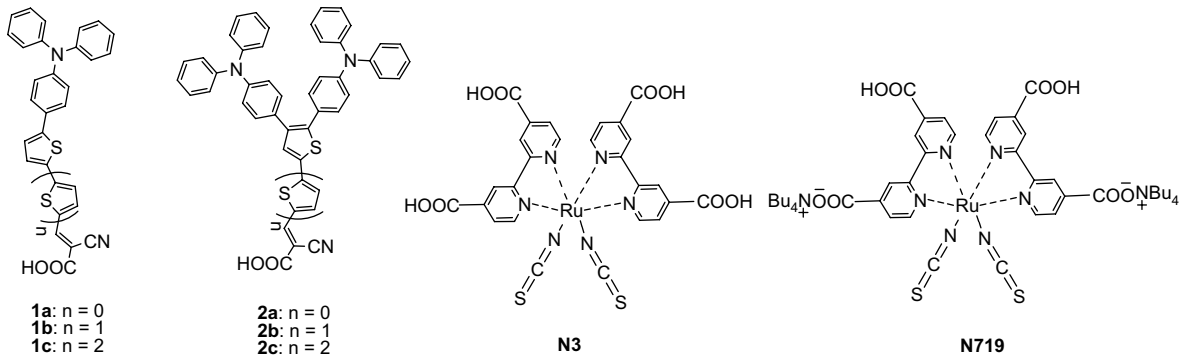

Fig. 1. Chemical structures of the novel dyes, **N3**, and **N719**.

2. Results and discussion

2.1. Structural design consideration

The chemical structures of the bis-TPA substituted dye molecules **2a**–**c** are shown in Fig. 1. The dye molecules are composed of three parts: (1) bis-TPA donating groups; (2) an oligothiophene bridge; and (3) a cyanoacrylic acid anchoring group. This type of structural design is based on the following considerations: (1) the bis-TPA groups may not only enhance the electron-donating ability, but also effectively inhibit I_3^- from approaching the surface of nanocrystallite TiO_2 film by the formation of a denser dye layer at the surface of the TiO_2 film; (2) the oligothiophene bridge usually has very good chemical and environmental stability [14]; and the absorption spectra of the dye molecules can be easily tuned by changing the length of oligothiophene bridge; (3) the cyanoacrylic acid acts as the acceptor and the anchoring group. For a comparison, dye molecules carrying mono-TPA donor group **1a**–**c** as shown in Fig. 1 were also designed and synthesized.

2.2. Synthesis of the dye molecules

The synthetic route leading to the mono- and bis-TPA substituted dyes is shown in Fig. 2. Mono-TPA substituted dyes **1a**–**c** were synthesized by following literature procedures [13]. Suzuki–Miyaura cross-coupling of triphenylamine mono boronic acid pinacol ester **3** [27] and aldehydes **4a**–**c** [29] with tetrakis (triphenylphosphine)palladium(0) $Pd(PPh_3)_4$ [31] (ed. Note: May cause eye, skin, and respiratory tract irritation; the toxicological properties of this material have not been fully investigated) as the catalyst precursor in a biphasic mixture of aqueous $NaHCO_3$ and THF afforded the triphenylamine terminated (oligo)thiophene aldehydes **5a**–**c** [13], respectively, in yields of 95%, 90% and 93%. Knoevenagel condensation of **5a**–**c** and 2-cyanoacetic acid gave the desired dyes **1a**–**c** in yields of 85%, 66% and 60%, respectively. Suzuki–Miyaura cross-coupling of 2,3-dibromothiophene **6** [30] and a twofold excess of triphenylamine mono boronic acid pinacol ester **3** was carried out with $Pd(PPh_3)_4$ as the catalyst precursor in a biphasic mixture of aqueous $NaHCO_3$ and THF to afford the bis-TPA substituted thiophene **7** in a yield of 81%. The treatment of **7** in THF with *n*-BuLi at −78 °C yielded the corresponding 2-thienyllithium, which was subsequently quenched with tri-*iso*-propyl borate to afford the corresponding boronic acid. The reaction of the crude boronic acid with pinacol in methylene chloride under reflux yielded compound **8** in a 48% yield. Quenching of 4,5-bis (triphenylamine)-2-thienyl anion with DMF instead of tri-*iso*-propyl borate afforded **9a** in an 83% yield.

Suzuki–Miyaura cross-coupling of compound **8** with **4a** and **4b** under modified conditions with tris[tri(2-thienyl)phosphine]-palladium(0), $Pd(PTh_3)_3$ (ed. Note: May cause eye, skin and respiratory tract irritation; the toxicological properties of this material have not been fully investigated) as the catalyst precursor in a biphasic mixture of aqueous $NaHCO_3$ and THF afforded the corresponding aldehyde **9b** and **9c** in yields of 86% and 80%, respectively. The use of $Pd(PTh_3)_3$ as the catalyst precursor instead of $Pd(PPh_3)_4$ in Suzuki–Miyaura cross-coupling of thiophene-based monomers always gives improved yield [31]. Knoevenagel condensation of **9a**–**c** with 2-cyanoacetic acid yielded the desired bis-TPA substituted dyes **2a**–**c** in yields of 65%, 40% and 42%, respectively. The structures of all dye molecules were characterized

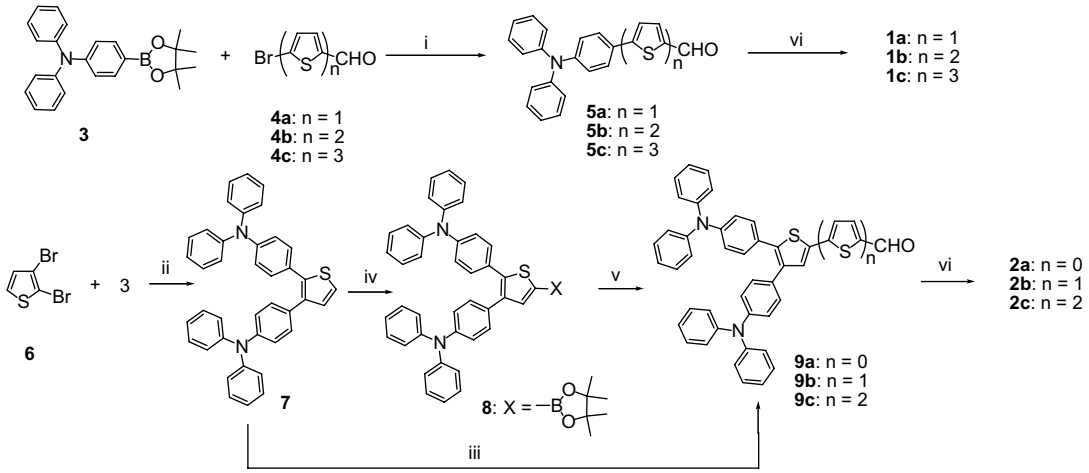

Fig. 2. Synthesis of the mono- and bis-TPA substituted dyes.

unambiguously with ^{1}H and ^{13}C NMR spectroscopy as well as matrix-assisted laser desorption ionization time-of-flight (MALDI-TOF) mass spectroscopy.

2.3. Optical properties of the dyes

The absorption spectra of all of the dye molecules (**1a–c** and **2a–c**) in dilute THF solutions at a concentration of 2×10^{-5} mol dm^{-3} are shown in Fig. 3. All dyes exhibited broad absorption spectra ranging from 270 to 570 nm mono-TPA-based dyes **1a–c** have a broad and strong absorption in the blue region with maxima at 432, 448, and 458 nm, respectively. Bis-TPA-based dyes **2a–c** exhibit two intense absorptions in the ultraviolet region and one in the visible region. Usually, the absorption bands at around 300 nm can be attributed to the π–π^* transition and bands at around 450 nm to the intramolecular charge transfer (ICT) between the donor and the acceptor [10–13]. The absorption bands arising from ICT slightly red-shifted with the introduction of more thiophene units due to the expansion of the π conjugation length. The molar extinction coefficients of **2a**, **2b** and **2c** are 18,000 dm^3 mol^{-1} cm^{-1} (at 430 nm), 27,900 dm^3 mol^{-1} cm^{-1} (at 443 nm), and 40,600 dm^3 mol^{-1} cm^{-1} (at 456 nm), respectively; whereas, those of **1a**, **1b**, and **1c** are 23,400 dm^3 mol^{-1} cm^{-1} (at 432 nm), 28,200 dm^3 mol^{-1} cm^{-1} (at 448 nm), 30,400 dm^3 mol^{-1} cm^{-1} (at 459 nm), respectively. The detailed results are summarized in Table 1. These numbers are obviously larger than that of **N3** (14,200 dm^3 mol^{-1} cm^{-1}) [32] indicating that the novel dyes have good light harvesting ability, and the chemical structure of **N3** is showing in Fig. 1. For both mono- and bis-TPA substituted dyes, the molar extinction coefficient increases with the increase of the length of oligothiophene spacers. Similar phenomena were also observed by Tsai [12] and Thomas [13].

2.4. Electrochemical properties

Highly efficient DSSCs require that the LUMO level of the dye molecules should be more negative than the conduction band edge of TiO_2 (E_{cb}) to ensure an effective electron injection from the dye molecules to the conduction band of the TiO_2 film and the HOMO level of the dye should be more positive than the redox potential of I_3^-/I^- to ensure the regeneration of dye molecules [33]. The HOMO levels of the dye molecules were estimated from the cyclic voltammetry curves. The zeroth–zeroth transition E_{0-0} values were estimated from the cross-point of the normalized UV absorption and photoluminescence spectra; the LUMO levels of the dyes were calculated according to the following equation:

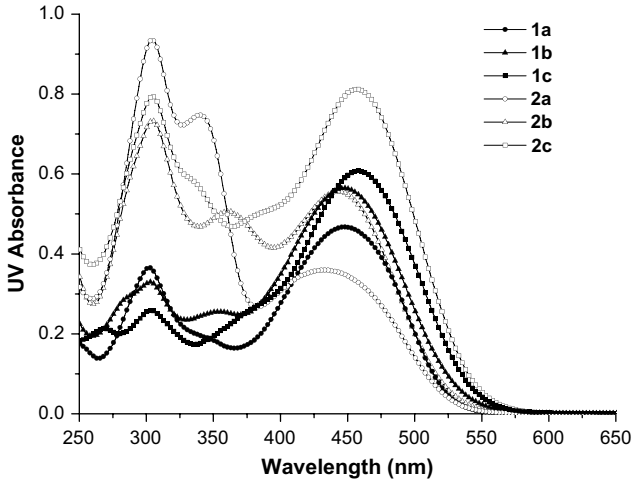

Fig. 3. UV–vis absorption spectra of dyes in THF solutions (2×10^{-5} mol dm^{-3}).

Table 1
Absorbance, emission, and electrochemical properties of dyes.

Dye	Absorbance[a]		Emission[a]			
	λ_{max} (nm)	ε at $\lambda_{max.}$ (dm^3 mol^{-1} cm^{-1})	$\lambda_{max.}$ (nm)	E_{0-0} (V) (abs/em)[b]	E_{ox} (V vs NHE)[c]	E_{LUMO} (V vs NHE)
1a	432	23400	568	2.415	1.178	1.238
1b	448	28200	567	2.402	1.130	1.272
1c	459	30400	566	2.392	1.020	1.372
2a	430	18000	570	2.507	1.186	1.321
2b	443	27900	572	2.425	1.184	1.241
2c	456	40600	570	2.399	1.146	1.253

[a] Absorption and emission spectra were measured in THF solutions (2×10^{-5} mol dm^{-3}).
[b] The zeroth–zeroth transition E_{0-0} values were estimated from the intersection of the absorption and emission spectra.
[c] Cyclic voltammetry of the oxidation behavior of the dyes was measured in dry acetonitrile containing 0.1 mol dm^{-3} tetrabutylammonium hexafluorophosphate ($TBAPF_6$) as supporting electrolyte (working electrode, glassy carbon; reference electrode, Ag/Ag^+ calibrated with ferrocene/ferrocenium (Fc/Fc^+) as an internal reference; counter electrode, Pt).

$E_{LUMO} = E_{HOMO} - E_{0-0}$; and the results are also summarized in Table 1. The LUMO levels of all dyes are more negative than the E_{cb} of TiO_2 (−0.5 V vs NHE) and the HOMO potential are more positive than the redox potential of I_3^-/I^- (∼0.4 V vs NHE). These results clearly demonstrate that the novel dyes are potentially efficient dyes for DSSCs. The HOMO levels of all dyes decrease with the introduction of more thiophene units (**1a** > **1b** > **1c** and **2a** > **2b** > **2c**); The HOMO levels of bis-TPA substituted dyes (**2a–c**) are more positive than those of mono-TPA (**1a–c**) substituted dyes, which might have a positive effect on the power conversion efficiency.

2.5. Photovoltaic performance of the dyes

The photovoltaic data are summarized in Table 2, and the corresponding photocurrent–voltage curves are shown in Fig. 4. As shown in Table 2, bis-TPA substituted dyes have higher open-circuit voltages (V_{oc}) than the corresponding mono-TPA substituted dyes and the improvements of V_{oc} for **2a–c** are 76, 86, and 61 mV, respectively. For both mono- and bis-TPA substituted dyes, the V_{oc} decreases slightly with the increase of the conjugation length. The increase of V_{oc} is attributed to the retardation of charge recombination at the nanocrystallite/dye/redox electrolyte interface [22,23]. This retardation may be caused by the following three aspects. Firstly, two hydrophobic TPA groups at the head of organic dyes may effectively inhibit the approach of I_3^- to the surface of nanocrystallite film. Secondly, a larger physical separation of the dye cation from the nanocrystallite film surface created by the bis-TPA functional groups on bis-TPA substituted dyes is the main reason for this retardation. Thirdly, the more positive HOMO levels of bis-TPA substituted dyes produce a larger driving force for the dye cation regeneration and hence reduce the back current. As shown in Table 2, the photovoltaic studies also confirm that bis-TPA substituted dyes are superior to the corresponding mono-TPA substituted dyes regarding to the energy conversion efficiency. The power conversion efficiencies of bis-TPA substituted dyes are

Table 2
DSSCs performance data of novel dyes.

Dye	I_{sc} (mA cm^{-2})	V_{oc} (V)	FF	η (%)
1a	7.84 ± 0.40	0.601 ± 0.004	0.73 ± 0.01	3.40 ± 0.16
1b	8.79 ± 0.40	0.600 ± 0.006	0.76 ± 0.01	4.02 ± 0.19
1c	6.40 ± 0.37	0.562 ± 0.010	0.73 ± 0.01	2.64 ± 0.11
2a	7.50 ± 0.50	0.678 ± 0.003	0.75 ± 0.02	3.77 ± 0.12
2b	9.88 ± 0.37	0.669 ± 0.009	0.74 ± 0.01	4.88 ± 0.18
2c	8.66 ± 0.18	0.610 ± 0.002	0.76 ± 0.01	4.01 ± 0.17
N3	14.22 ± 0.30	0.678 ± 0.020	0.69 ± 0.01	6.63 ± 0.07

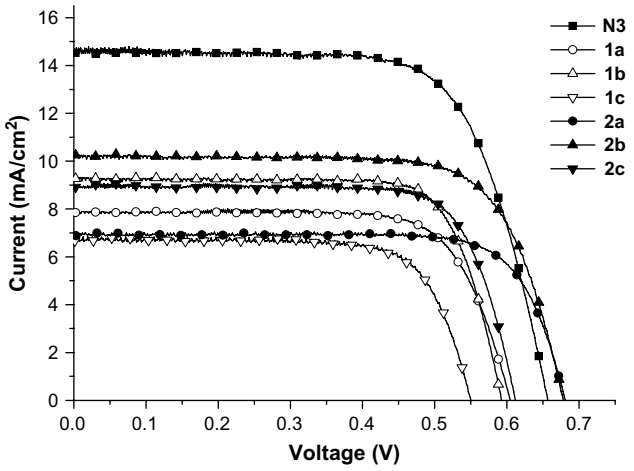

Fig. 4. Photocurrent–voltage curves of dyes sensitized TiO_2 electrodes.

higher than those of the corresponding mono-TPA substituted dyes is probably due to the fact that bis-TPA substituted dyes have a better light harvesting ability. A larger V_{oc} is also a prerequisite for higher power conversion efficiencies of these bis-TPA substituted dyes. The power conversion efficiencies of the bis-TPA substituted dyes are higher than those of the corresponding mono-TPA substituted dyes, especially for **2c** which has a 52% improvement in comparison to the corresponding dye **1c**. For the novel dyes, **2b** has the highest power conversion efficiency up to 5.06%. Under the same experimental conditions, the fill factors of novel dyes are even better than that of **N3**.

2.6. Computer simulation of molecular orbital

The molecular geometries and electron distributions of **2a–c** were obtained by using density function theory (DFT) calculations with Gaussian 03 program. The calculations were performed with the B3LYP exchange correlation functional under 3-21G(d) basis and the results are displayed in Fig. 5. The electron distribution before the light irradiation locates mainly on the donor units; whereas after light irradiation it moves to the acceptor units close to the anchoring groups, which favors the electron injection from the dye molecules to the conduction band edge of TiO_2.

3. Conclusions

Three, novel, donor-acceptor dyes that posses a supplementary non-conjugating donor group were designed and synthesized. A solar energy to electricity conversion efficiency of 5.06% is achieved for the bis-TPA substituted dye **2b**, which is significantly higher than the corresponding mono-TPA substituted donor-acceptor dye **1b**. The higher efficiency of bis-TPA substituted dyes is mainly

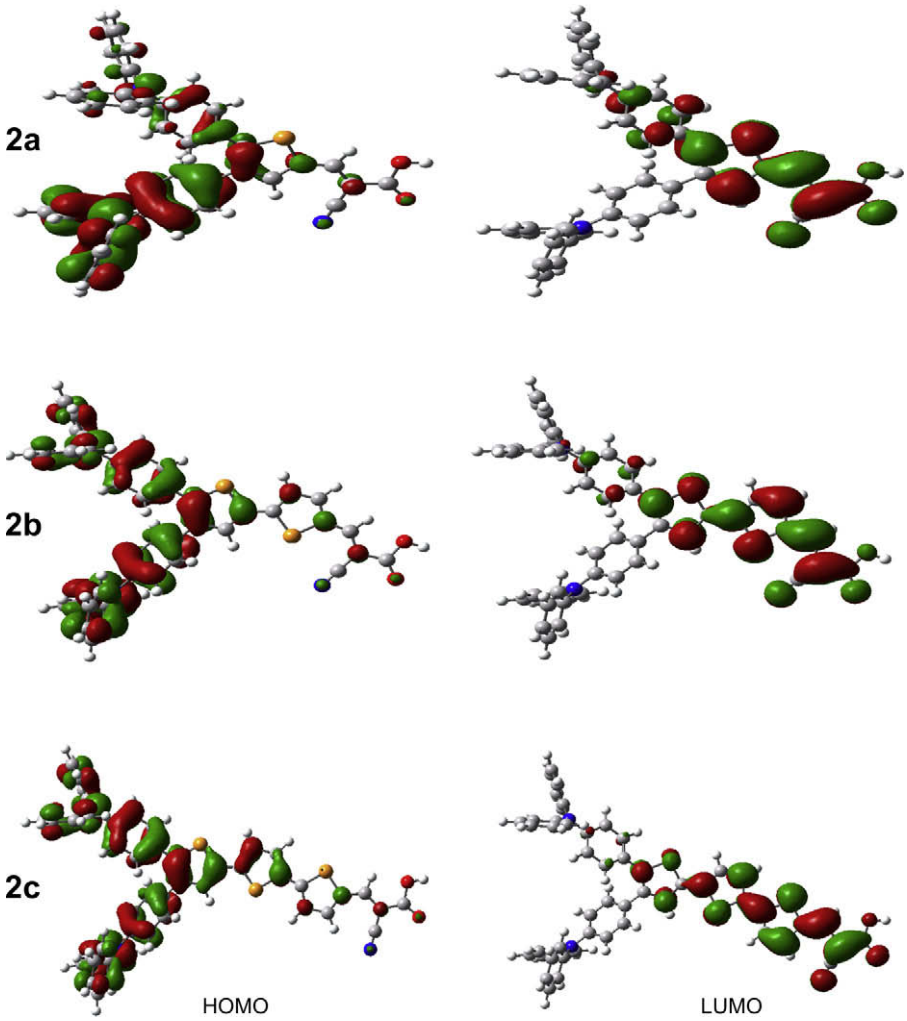

Fig. 5. The frontier orbitals of **2a–c** optimized with DFT at the B3LYP/3-21G(d) level.

attributed to their higher V_{oc}. The two hydrophobic TPA groups at the head of organic dyes could effectively inhibit the approaching of I_3^- to the surface of nanocrystallite film. Detailed experiments and the investigation of the interfacial charge transfer processes of these dyes are in progress aiming to further increase the performance of DSSCs fabricated with this new group of dyes.

4. Experimental section

4.1. Assembly and characterization of DSSCs

Nanocrystalline TiO_2 films were deposited on the fluorine-doped SnO_2 conducting glass substrate (15 Ω cm^{-2}) by screen-printing a TiO_2 (Degussa P25) paste. The thickness of film was controlled to be about 15 μm by repeating screen-printing the paste. The TiO_2 films was heated to 450 °C and sintered for 30 min, then cooled to ~80 °C and immersed into the dye solutions (0.3 mmol dm^{-3} dyes in dry THF containing 10 mmol dm^{-3} 3α,12α-dihydroxy-5β-cholanic acid) at room temperature for at least 12 h. The electrolyte consisted of 0.6 mol dm^{-3} methylhexylimidazolium iodide, 0.05 mol dm^{-3} iodine, 0.1 mol dm^{-3} LiI and 0.5 mol dm^{-3} *tert*-butylpyridine in 3-methoxypropionitrile. An open sandwich-type cell, which was not sealed, was fabricated in air by clamping the sensitized TiO_2, a drop of electrolyte and a thermally platinized FTO counter electrode with two clips. The active electrode area was 0.15 cm^2.

The photocurrent–photovoltage measurements were recorded by a potentiostat (Princeton Applied Research, Model 263A). A solar light simulator (Oriel, 91192) was used as the white light source to give AM 1.5 illumination on the surface of the solar cells. The intensity of incident light was measured with a radiant power/energy meter (Oriel, 70260) before each experiment.

4.2. Cyclovoltagram

The electrochemical properties of these dyes were investigated with a standard three-electrode electrochemical cell in acetonitrile solution containing 0.1 mol dm^{-3} tetrabutylammonium hexafluorophosphate ($TBAPF_6$) at room temperature with a scanning rate of 20 mV s^{-1}. The oxidation potentials of these dyes were measured vs $Ag/AgNO_3$ as the reference electrode and a standard ferrocene/ferrocenium redox system as the internal standard for estimating the HOMO levels of the dye films.

4.3. Materials and instruments

All chemicals were purchased from commercial suppliers and used without further purification. *N*-(4-(4,4,5,5-tetramethyl-1,3,2-dioxaborolan-2-yl)phenyl)-*N*-phenylbenzenamine, 2,3-dibromothiophene, 5-bromothiophene-2-carbaldehyde, and 5-(5-bromothiophen-2-yl)thiophene-2-carbaldehy-de were prepared according to literature procedures [27,28,30]. The catalyst precursor $Pd(PPh_3)_4$ was prepared according to the literature [29], and stored in a Schlenk tube under nitrogen. Solvents were dried according to standard procedures. All reactions were performed under an atmosphere of nitrogen and monitored by TLC with silica gel 60 F254 (Merck, 0.2 mm). Column chromatography was carried out on silica gel (200–300 mesh). ^1H and ^{13}C NMR spectra were recorded on a Bruker AV400 spectrometer in $CDCl_3$ or DMSO. Electronic absorption spectra were obtained on a SHIMADZU UV–visible spectrometer model UV-1601PC. Fluorescence spectra were recorded on a Varian FLR025. Elemental analyses were performed on a Flash EA 1112 analyzer. The matrix-assisted laser desorption ionization time-of-flight (MALDI-TOF) MS spectra were obtained on a Bruker BIFLEXIII mass spectrometer.

4.4. Synthesis

4.4.1. 2,3-bis[4-(diphenylamino)phenyl]thiophene (**7**)

A mixture of 2,3-dibromothiophene **6** (919 mg, 3.8 mmol), *N*-(4-(4,4,5,5-tetramethyl-1,3,2-dioxaborolan-2-yl)phenyl)-*N*-phenylbenzenamine **3** (3.1 g, 8.36 mmol), $NaHCO_3$ (4.8 g, 57 mmol), $Pd(PPh_3)_4$ (66 mg, 57 μmol), THF (30 mL), and water (10 mL) in a Schlenk flask was carefully degassed and charged with nitrogen. The mixture was stirred and refluxed for 24 h under N_2. CH_2Cl_2 (20 mL) was then added; the organic layer was separated; the aqueous layer was extracted by CH_2Cl_2 for three times (20 mL×3); and the combined organic layers were dried over anhydrous Na_2SO_4 and evaporated to dryness. The residue was purified by column chromatography on silica gel eluting with CH_2Cl_2/petroleum (1:3, v:v) to afford **7** as a brown solid (1.76 g, 81%). ^1H NMR (400 MHz, $CDCl_3$): δ 7.22–7.16 (m, 13H), 7.10–7.01 (m, 9H), 6.99–6.94 (m, 8H). ^{13}C NMR (100 MHz, $CDCl^3$): δ = 147.7, 147.6, 147.1, 146.6, 138.1, 137.3, 130.8, 130.4, 130.0, 129.9, 129.4, 129.3, 128.3, 124.8, 124.5, 123.4, 123.3, 123.2, 123.0, 122.8. Anal. Calcd for $C_{40}H_{30}N_2S$: C, 84.18; H, 5.30; N, 4.91. Found: C, 83.96; H, 5.45; N, 4.75.

4.4.2. 4,5-bis(4-(diphenylamino)phenyl)thiophene-2-carbaldehyde (***9a***)

A solution of **7** (942 mg, 1.65 mmol) in THF (40 mL) was cooled to −78 °C under nitrogen atmosphere. *n*-BuLi (0.73 mL, 2.5 M) was added dropwise and the mixture was stirred at −78 °C for 1 h. DMF (0.38 mL, 4.65 mmol) was added, and the mixture was stirred and allowed to warm to room temperature overnight. Aqueous hydrochloric acid was added; the organic layer was separated; the aqueous layer was extracted with CH_2Cl_2 for three times (20 mL×3); and the combined organic layers were dried over anhydrous Na_2SO_4 and evaporated to dryness. The residue was purified by column chromatography on silica gel eluting with CH_2Cl_2/petroleum (1:3, v:v) to afford **9a** as a yellow solid (816 mg, 83%). ^1H NMR (400 MHz, $CDCl_3$): δ 9.87 (s, 1H), 7.74 (s, 1H), 7.29–7.20 (m, 8H), 7.16–7.10 (m, 12H), 7.07–7.00 (m, 6H), 6.94 (d, J = 8.51 Hz, 2H). ^{13}C NMR (100 MHz, $CDCl_3$): δ 182.8, 148.7, 148.6, 147.6, 147.4, 147.2, 140.4, 139.5, 138.6, 129.9, 129.8, 129.1, 126.2, 125.4, 124.8, 123.9, 123.3, 123.0, 121.8. Anal. Calcd for $C_{41}H_{30}N_2O_2S$: C, 82.24; H, 5.05; N, 4.68; Found: C, 81.89; H, 5.66; N, 4.40.

4.4.3. N-*(4-(2-(4-(diphenylamino)phenyl)-5-(4,4,5,5-tetramethyl-1,3,2-dioxaborolan-2-yl)thiophen-3-yl)phenyl)*-N-*phenylbenzenamine (**8**)*

To a solution of **7** (1.32 g, 2.32 mmol) in THF (40 mL), which was already cooled to −78 °C under N_2, was added dropwise *n*-BuLi (1.02 mL, 2.5 M). The mixture was stirred at −78 °C for 1 h, and then tri-*iso*-propyl borate (0.54 mL, 4.64 mmol) was added. The mixture was allowed to warm to room temperature overnight. Aqueous hydrochloric acid was added; the organic layer was separated; the aqueous layer was extracted with ether for three times (20 mL×3); and the combined organic layers were dried over anhydrous Na_2SO_4 and evaporated to dryness. The resulted boronic acid was dissolved in anhydrous CH_2Cl_2 (60 mL), and pinacol (0.543 g, 4.64 mmol) was added. The mixture was refluxed for 5 h with a Dean–Stark apparatus to remove the formed H_2O. After the removal of the solvent, the residue was purified by column chromatography on silica gel eluting with EtOAc/hexane (1:5, v:v) to afford **8** as a brown solid (0.78 g, 48%). ^1H NMR (400 MHz, $CDCl_3$): δ 7.65 (s, 1H), 27–7.16 (m, 12H), 7.15 (t, J = 7.13, 8H), 7.05–6.93 (m, 8H), 1.35 (s, 12H). ^{13}C NMR (100 MHz, $CDCl_3$): δ 146.6, 146.3, 146.2, 145.4, 144.2, 139.5, 137.6, 129.6, 128.8, 128.7, 128.3, 128.2, 128.2, 128.1, 126.9, 123.8, 123.4, 122.2, 121.7, 121.4, 83.1, 23.7. Anal. Calcd for $C_{46}H_{41}BN_2O_2S$: C, 79.30; H, 5.93; N, 4.02; Found: C, 79.02; H, 6.00; N, 3.96.

*4.4.4. Compounds **9b–c***

A mixture of **8** (0.5 mmol),5-bromothiophene-2-carbaldehyde **4a** or 5-(5-bromothiophen-2-yl)thiophene-2-carbaldehyde **4c** (0.5 mmol), $NaHCO_3$ (7.5 mmol), $Pd(PTh_3)_3$ (8 mg, 7.5 μmol), THF (30 mL), and water (12 mL) in a Schlenk flask was carefully degassed and charged with nitrogen. The mixture was stirred and refluxed for 24 h. The mixture was extracted with CH_2Cl_2 (20 mL×3); the combined organic layers were dried over anhydrous Na_2SO_4 and evaporated to dryness. The residue was purified by column chromatography on silica gel eluting with CH_2Cl_2/petroleum (1:3, v:v) to afford **9b–c**.

*4.4.4.1. 5-(4,5-bis(4-(diphenylamino)phenyl)-thio-phen-2-yl)thiophene-2-carbaldehyde (**9b**).* Yield: 86%; an orange solid. ^{1}H NMR (400 MHz, $CDCl_3$): δ 9.85 (s, 1H), 7.67 (d, J = 3.43, 1H), 7.28–7.17 (m, 14H), 7.12–7.10 (d, 8H), 7.07–6.99 (m, 6H), 6.98 (d, J = 7.96, 2H). ^{13}C NMR (100 MHz, $CDCl_3$): δ 182.5, 147.8, 147.6, 147.4, 147.2, 141.6, 140.1, 138.5, 137.5, 133.3, 129.8, 129.7, 129.5, 129.4, 126.9, 125.1, 124.8, 123.9, 123.6, 123.2, 123.1, 122.3. Anal. Calcd for $C_{45}H_{32}N_2OS_2$: C, 79.38; H, 4.74; N, 4.11; Found: C, 79.02; H, 4.86; N, 4.33.

*4.4.4.2. 5-(5-(4,5-bis(4-(diphenylamino)phenyl)thiophen-2-yl)thiophen-2-yl)thiophene-2-carbaldeh-yde (**9c**).* Yield: 80%; a red solid. ^{1}H NMR (400 MHz, $CDCl_3$): δ 9.85 (s, 1H), 7.66 (d, J = 3.49, 1H), 7.28–7.18 (m, 16H), 7.12–7.10 (d, 8H), 7.06–6.99 (m, 6H), 6.95 (d, J = 8.15, 2H). ^{13}C NMR (100 MHz, $CDCl_3$): δ 182.5, 147.7, 147.5, 147.4, 147.0, 141.7, 138.2, 137.4, 130.1, 129.8, 129.5, 129.4, 127.8, 127.1, 125.0, 124.7, 124.4, 124.1, 123.5, 123.2, 122.5. Anal. Calcd for $C_{49}H_{34}N_2OS_3$: C, 77.13; H, 4.49; N, 3.67; Found: C, 76.80; H, 4.54; N, 3.85.

*4.4.5. Compounds **2a–c***

A mixture of **9a** (82 mg, 0.14 mmol), **9b** (90 mg, 0.13 mmol) or **9c** (78 mg, 0.10 mmol), cyanoacetic acid (70 mg, 0.82 mmol; 45 mg, 0.52 mmol or 53 mg, 0.60 mmol), piperidine (0.5 mL), dry $CHCl_3$ (10 mL), and dry CH_3CN (10 mL) was refluxed for 12 h under nitrogen atmosphere. CH_2Cl_2 (50 mL) was added; the organic layer was washed successively with water (10 mL×3) and brine (10 mL×3), dried over anhydrous $MgSO_4$, and evaporated to dryness. The residue was purified by column chromatography on silica gel eluting with CH_2Cl_2 increasing gradually to CH_2Cl_2/CH_3OH (1:1, v:v) to afford **2a–c**.

*4.4.5.1. 3-(4,5-bis(4-(diphenylamino)phenyl)thiophen-2-yl)-2-cyanoacrylic acid (**2a**).* Yield: 65%; a dark red solid. ^{1}H NMR (400 MHz, $CDCl_3$): δ 8.31 (s, 1H), 7.81 (s, 1H), 7.31–7.23 (m, 8H), 7.16–7.09 (m, 12H), 7.07–7.00 (m, 6H), 6.94 (d, J = 8.63, 2H). ^{13}C NMR (100 MHz, $CDCl_3$): δ 166.6, 150.5, 148.9, 147.6, 147.5, 147.0, 141.6, 139.3, 132.8, 130.1, 130.0, 129.8, 129.6, 129.5, 128.4, 125.6, 125.5, 124.9, 124.1, 123.4, 122.9, 121.6, 115.9, 96.3. m/z (MALDI-TOF): $[M]^+$ calcd for $C_{44}H_{31}N_3O_2S$ 665.2. Found, 665.0.

*4.4.5.2. 3-(5-(4,5-bis(4-(diphenylamino)phenyl)thiophen-2-yl)thiophen-2-yl)-2-cyanoacrylic acid (**2b**).* Yield: 40%; a dark solid. ^{1}H NMR (400 MHz, DMSO): δ 8.12 (s, 1H), 7.59 (s, 1H), 7.46 (s, 1H), 7.39 (s, 1H), 7.28–7.21 (m, 8H), 7.14 (d, J = 8.04, 2H), 7.10 (d, J = 8.04, 2H), 7.06–6.99 (m, 4H), 6.97–6.95 (d, 8H), 6.83 (d, J = 8.14, 2H), 6.77 (d, J = 8.19, 2H). ^{13}C NMR (100 MHz, DMSO): δ = 164.1, 147.0, 146.9, 146.6, 146.4, 137.9, 137.7, 135.5, 133.1, 129.7, 129.6, 129.5, 129.4, 129.2, 128.5, 126.2, 124.7, 124.4, 124.2, 123.7, 123.2, 122.5, 121.6, 118.9. m/z (MALDI-TOF): $[M]^+$ calcd for $C_{48}H_{33}N_3O_2S_2$ 747.2. Found, 747.8.

*4.4.5.3. 3-(5-(5-(4,5-bis(4-(diphenylamino)pheny-l)-thiophen-2-yl)thiophen-2-yl)thiophen-2-yl)-2-cyanoacrylic acid (**2c**).* Yield: 42%; a dark solid. ^{1}H NMR (400 MHz, DMSO): δ 8.23 (s, 1H), 7.74 (s, 1H), 7.42 (d, J = 7.32, 3H), 7.31–7.22 (m, 9H), 7.16 (d, J = 8.01, 2H), 7.11 (d, J = 8.11, 2H), 7.07–6.98 (m, 12H), 6.85 (d, J = 8.10, 2H), 6.80 (d, J = 8.14, 2H). ^{13}C NMR (100 MHz, DMSO): δ 164.2, 147.4, 147.1, 146.9, 143.1, 138.2, 137.8, 137.2, 135.6, 134.5, 133.8, 130.2, 130.1, 129.9, 127.8, 126.9, 125.8, 125.2, 124.7, 124.2, 123.8, 123.1, 122.3, 118.7, 105.4. m/z (MALDI-TOF): $[M]^+$ calcd for $C_{52}H_{35}N_3O_2S_3$ 829.2. Found, 829.1.

Acknowledgements

Financial support by the NSF of China (20774099, 20673141, 20834006 and 50521302), 863 Program (2006AA03Z341 and 2008AA05Z425), and the Open Project of State Key Laboratory of Supramolecular Structure and Materials (SKLSSM200706) is gratefully acknowledged.

References

[1] O'Regan B, Grätzel M. A low-cost high-efficiency solar cell based on dye-sensitized colloidal TiO_2 film. Nature 1991;353:737–9.
[2] Liu X, Luo Y, Li H, Fan Y, Yu Z, Lin Y, et al. Room temperature fabrication of porous ZnO photoelectrodes for flexible dye-sensitized solar cells. Chemical Communications 2007:2847–9.
[3] Nazeeruddin MK, Angelis FD, Fantacci S, Selloni A, Viscardi G, Liska P, et al. Combined experimental and DFT-TDDFT computational study of photoelectrochemical cell ruthenium sensitizers. Journal of the American Chemical Society 2005;127(48):16835–47.
[4] Nazeeruddin MK, Péchy P, Renouard T, Zakeeruddin SK, Humphry-Baker R, et al. Engineering of efficient panchromatic sensitizers for nanocrystalline TiO_2-based solar cells. Journal of the American Chemical Society 2001;123(8):1613–24.
[5] Hara K, Sato T, Katoh R, Furube A, Ohga Y, Shinpo A, et al. Molecular design of coumarin dyes for efficient dye-sensitized solar cells. Journal of Physical Chemistry B 2003;107(2):597–606.
[6] Sayama K, Hara K, Mori N, Satsuki M, Suga S, Tsukagoshi S, et al. Photosensitization of a porous TiO_2 electrode with merocyanine dyes containing a carboxyl group and long alkyl chain. Chemical Communications 2000:1173–4.
[7] Ehret A, Stuhl L, Spitler M. T. Spectral sensitization of TiO_2 nanocrystalline electrodes with aggregated cyanine dyes. Journal of Physical Chemistry B 2001;105(41):9960–5.
[8] Horiuchi T, Miura H, Sumioka K, Uchida S. High efficiency of dye-sensitized solar cells based on metal-free indoline dyes. Journal of the American Chemical Society 2004;126(39):12218–9.
[9] Wang Z, Li F, Huang C. Highly efficient sensitization of nanocrystalline TiO_2 with styryl benzothiazolium propylsulfonate. Chemical Communications 2000:2063–4.
[10] Liang M, Xu W, Cai F, Chen P, Peng B, Chen J, et al. New triphenylamine-based organic dyes for efficient dye-sensitized solar cells. Journal of Physical Chemistry C 2007;111(11):4465–72.
[11] Velusamy M, Thomas KRJ, Lin JT, Hsu Y, Ho K. Organic dyes incorporating low-band-gap chromophores for dye-sensitized solar cells. Organic Letters 2005;7(10):1899–902.
[12] Tsai M, Hsu Y, Lin JT, Chen H, Hsu C. Organic dyes containing 1H-phenanthro[9,10-*d*]imidazole conjugation for solar cells. Journal of Physical Chemistry C 2007;111(50):18785–93.
[13] Thomas KRJ, Hsu Y, Lin JT, Lee K, Ho K, Lai C, et al. 2,3-disubstituted thiophene-based organic dyes foe solar cells. Chemistry of Materials 2008;20(15):1830–40.
[14] Hara K, Sato T, Katoh R, Furube A, Yoshihara T, Murai M, et al. Novel conjugated organic dyes for efficient dye-sensitized solar cells. Advanced Functional Materials 2005;15(2):246–52.
[15] Kim S, Lee JK, Kang SO, Ko J, Yum J, Fantacci S, et al. Molecular engineering of sensitizers for solar cell applications. Journal of the American Chemical Society 2006;128(51):16701–7.
[16] Choi H, Lee JK, Song K, Kanga SO, Ko J. Novel organic dyes containing bis-dimethylfluorenyl amino benzo[*b*]thiophene for highly efficient dye-sensitized solar cell. Tetrahedron 2007;63(15):3115–21.
[17] Tian H, Yang X, Chen R, Pan Y, Li L, Hagfeldt A, et al. Phenothiazine derivatives for efficient organic dye-sensitized solar cells. Chemical Communications 2007:3741–3.
[18] Chen R, Yang X, Tian H, Sun L. Tetrahydroquinoline dyes with different spacers for organic dye-sensitized solar cells. Journal of Photochemistry and Photobiology A: Chemistry 2007;189:295–300.
[19] Koumura N, Wang Z, Mori S, Miyashita M, Suzuki E, Hara K. Alkyl-functionalized organic dyes for efficient molecular photovoltaics. Journal of the American Chemical Society 2006;128(44):14256–7.
[20] Huang SY, Schlichthörl G, Nozik AJ, Grätzel M, Franke AJ. Charge recombination in dye-sensitized nanocrystalline TiO_2 solar cells. Journal of Physical Chemistry B 1997;101(14):2576–82.
[21] Smestad G. Testing of dye sensitized TiO_2 solar cells: theoretical voltage output and photoluminescence efficiencies. Solar Energy Materials and Solar Cells 1994;32(3):273–88.
[22] Satoh N, Nakashima T, Yamamoto K. Metal-assembling dendrimers with a triarylamine core and their application to a dye-sensitized solar cell. Journal of the American Chemical Society 2005;127(37):13030–8.

[23] Palomares E, Clifford JN, Haque SA, Lutz T, Durrant JR. Control of charge recombination dynamics in dye sensitized solar cells by the use of conformally deposited metal oxide blocking layers. Journal of the American Chemical Society 2003;125(2):475–82.
[24] Bonhôte P, Moser J, Humphry-Baker R, Vlachopoulos N, Zakeeruddin SM, Walder L, et al. Long-lived photoinduced charge separation and redox-type photochromism on mesoporous oxide films sensitized by molecular dyads. Journal of the American Chemical Society 1999;121(6):1324–36.
[25] Clifford JN, Yahioglu G, Milgrom LR, Durrant JR. Molecular control of recombination dynamics in dye sensitized nanocrystalline TiO_2 films. Chemical Communications 2002:1260–1.
[26] Haque SA, Handa S, Peter K, Palomares E, Thelakkat M, Durrant JR. Supermolecular control of charge transfer in dye-sensitized nanocrystalline TiO_2 films: towards a quantitative structure–function relationship. Angewandte Chemie International Edition 2005;44(35):5740–4.
[27] Sun M, Li J, Li B, Fu Y, Bo Z. Toward high molecular weight triphenylamine-based hyperbranched polymers. Macromolecules 2005;38(7):2651–8.
[28] Yang F, Xu X, Gong Y, Qiu W, Sun Z, Zhou J, et al. Synthesis and nonlinear optical absorption properties of two new conjugated ferrocene-bridge-pyridinium compounds. Tetrahedron 2007;63(37):9188–94.
[29] Tolman CA, Seidel WC, Gerlach DH. Thiarylphosphine and ethylene complexes of zerovalent nickel, palladium, and platinum. Journal of the American Chemical Society 1972;94(8):2669–76.
[30] Antolini L, Goldoni F, Iarossi D, Mucci A, Schenetti L. Synthesis of 3,4-dibromo-2,2-bithiophene: a useful intermediate for 3,4-disubsitituted 2,2-bithiophenes. X-Ray molecular structure of 3,4-dibromo-2,2bithiophene. Journal of Chemical Society Perkin Transactions 1997;1:1957–62.
[31] Li W, Han Y, Li B, Liu C, Bo Z. Tri[tri(2-thienyl)phosphine]palladium as the catalyst precursor for thiophene-based Suzuki–Miyaura crosscoupling and polycondensation. Journal of Polymer Science Part A: Polymer Chemistry 2008;46:4556–63.
[32] Nazeeruddin MK, Kay A, Rodicio I, Humpbry-Baker R, Miiller E, Liska P, et al. Conversion of light to electricity by *cis*-X2bis(2,2-bipyridiyl-4,4-dicarboxylate)ruthenium(II) charge-transfer sensitizers ($X = Cl^-$, Br^-, I^-, CN^-, and SCN^-) on nanocrystalline titanium dioxide electrodes. Journal of the American Chemical Society 1993;115(14):6382–90.
[33] Kuang D, Ito S, Wenger B, Klein C, Moser J, Humphry-Baker R, et al. High molar extinction coefficient heteroleptic ruthenium complexes for thin film dye-sensitized solar cells. Journal of the American Chemical Society 2006;128(12):4146–54.